SiPM Classification of the Pre-Production GCT Camera of CTA

SiPM Klassifikation der Pre-Production GCT Kamera von CTA
Master-Thesis von Ben Gebhardt aus Heidelberg
Tag der Einreichung:

1. Gutachten: Dr. Richard White (MPIK)
2. Gutachten: Prof. Jim Hinton (MPIK)
3. Gutachten: Prof. Tetyana Galatyuk (TU DA)

TECHNISCHE
UNIVERSITÄT
DARMSTADT

Fachbereich Physik
Max Planck Institut f"ur Kernphysik Heidelberg

SiPM Classification of the Pre-Production GCT Camera of CTA
SiPM Klassifikation der Pre-Production GCT Kamera von CTA

Vorgelegte Master-Thesis von Ben Gebhardt aus Heidelberg

1. Gutachten: Dr. Richard White (MPIK)
2. Gutachten: Prof. Jim Hinton (MPIK)
3. Gutachten: Prof. Tetyana Galatyuk (TU DA)

Tag der Einreichung:
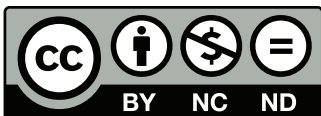
Erklärung zur Master-Thesis

Hiermit versichere ich, die vorliegende Master-Thesis ohne Hilfe Dritter nur mit den angegebenen Quellen und Hilfsmitteln angefertigt zu haben. Alle Stellen, die aus Quellen entnommen wurden, sind als solche kenntlich gemacht. Diese Arbeit hat in gleicher oder ähnlicher Form noch keiner Prüfungsbehörde vorgelegen.

Darmstadt, den March 6, 2017

_____

(B. Gebhardt)

1 Results

Preliminary results chapter
In this chapter, I will list the final results per device in a list of measured criteria. At the end I will conclude with a comparison between devices and to the results from other groups.

1.1 Hamamatsu S12642

The Silicon Photomultiplier by Hamamatsu Photonics designated S12642 is a 3 mm by 3 mm device. One array of pixels consists of 256 pixels, 4 of which are electrically tied togother to form a 6mm by 6mm superpixel respectively. This practise is necessary for the pre-production camera CHEC-S, because the focal plane is mechanically designed to house 64 6mm^2 pixels, connected to the TARGET modules. Furthermore I expect this to have an influence on my results due to electrical crosstalk, but this is only of minor concern due to the following. My measurements of the CHEC-S tile concentrate on the array as an as-is device. This means all results, influenced by external factors outside the actual SiPMs physics, are valid on the assumption, that the way I was conducting the measurements is the way the Photomultiplier will later be incorporated into the camera. On that ground, deviations of my results from the results of other groups and the manufacturer itself are expected. To clarify this further, I expect, for example, that the tests done at Hamamatsu Photonics

Figure 1: CHEC-S tile

where conducted on a single 3mm by 3mm pixel, not an array of 256 pixels, where 4 are tied together. Also divergence of shaping and amplification electronics between the groups will result in some differences. For this test, the CHEC-S tile is connected to the CHEC-S buffer, supplied with ±4V, where the signal is amplified. This signal in turn is then shaped via the CHEC-S shaper, iteration (XXXXXXX in devices chapter) by Luigi Tibaldo. This is done in order to lower the unshaped pulse from a FWHM in the 100s ns to 10ns. This whole amplification and shaping chain is simulating later usage in the TARGET modules.
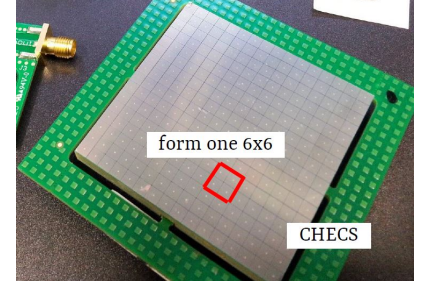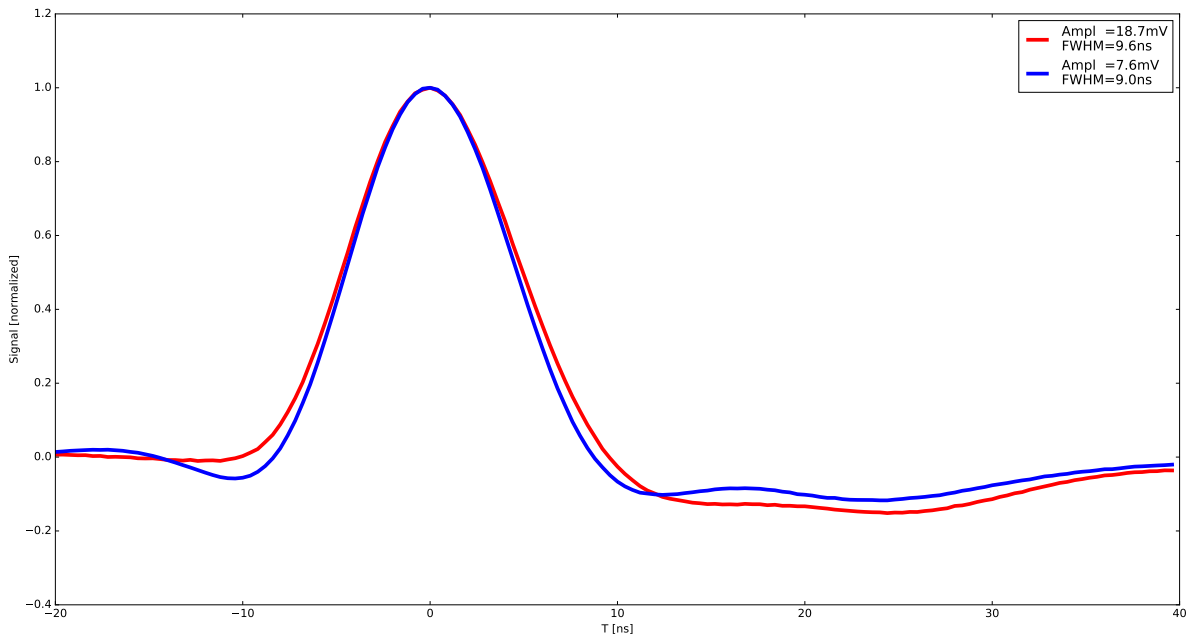

Figure 2: The average pulse shape of the 1photoelectron in blue and the 2photoelectron pulse in red of HPK S12642 at 25° C and 67.8V, which is around the proposed operating point. Both pulses are averaged over »1000 events and normalized to illustrate possible differences in pulseshape resulting from the utilized shaping electronics. Both pulses have a FWHM of around 10ns and are nearly free of ringing. The resulting average amplitude of the 1p.e. pulse is later used to calculate the Gain in [mV/p.e.] instead of [V*IntWin] by cross-referencing the 1p.e. amplitude at multiple bias-voltages.

1.1.1 Gain

As descibed above, the average pulse shape fig(2) is used to convert the relative gain from the analysis procedure to an absolute gain in sensible units. This is necessary, because the analysis aims to use pulse-area rather than -height. In Figure (3) (left) the relative gain is shown, the right side shows the gain after conversion. A lower gain with increasing temperature is expected and described in detail in the chapter (physics of SiPMs i guess). In short, increased lattice movement due to higher temperature hinders photoelectron transport. The effects visible at extreme bias-voltages at both ends are analysis related. The gain of a SiPM is expected to be linear over bias-voltage at a constant temperature. In the lower regime at Vb 66.5V my analysis method struggles to pick up pulses, because of the low gain compared to the noise. Depending on the chosen peak-finding threshold, I expect the analysis to interpret noise peaks as 1p.e. peaks at an increasing rate, the lower the overvoltage is. This is visible in the sudden break in linearity at 30° C and 35° C , where the gain is almost in a plateau, due to this effect. At the highest bias-voltages the influence of the noise is similar. The point at Vov 5V,which is way over the proposed point of operation at Vov 3V. The same threshold is again counting noise peaks as 1p.e. peaks, but due to the abundance of 1p.e. pulses this just results in an apparent lowering of the gain.
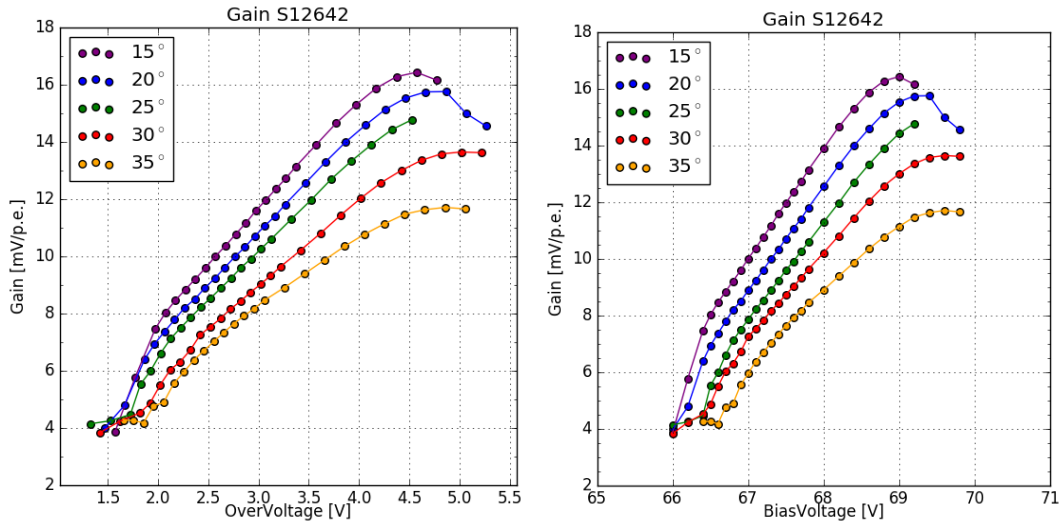

Figure 3: Gain of the HPK S12642 pixel, plotted against over- , bias-voltage and temperature.

1.1.2 Dark Count Rate

I expect the Dark Count Rate to increase with temperature, which is the case fig(4). I also expect it to follow a nearly linear progression, a sudden turn-up or turn-down of the Dark Count Rate would be analysis related. The turn-up at a certain point is visible in Figure (4), particulary for 15° C (purple) and 20° C (blue) respectively. At 15° C and an Overvoltage of 4V, the Dark Count Rate starts to deviate from the previously linear behaviour. It starts to rise more rapid than before, which I can attribute to the fact, that the Optical Cross Talk at that point is very high; higher than 50% fig(5) (left). I suspect that I do not reach this critical point for the higher temperatures of 25° C (green) and 30° C (red), so the effect is barely, if not at all visible. At 35° C (yellow) I suspect my analysis is not able to count every pulse, due to the high rate of 9-10 MHz. A majority of the pulses overlapping each other and being counted as a 2p.e. event rather than 2 1p.e. events would reduce the Dark Count Rate significantly. At this point, heating of the Silicon Photo-multipliers surface due to the high rate could also affect the Dark Count Rate through shifting the temperature slightly upwards, away from 35° C . So that the Dark Count Rate declared at 35° C is in reality the rate at higher temperatures.

At the lower end of the bias-voltage range, I suspect, that a major part of the found 1p.e. pulses are actually noise related. So the Dark Count Rate changing to a plateau is expected. This is also due to the fact, that my measurements are done with a fixed bias-voltage range. Due to the increase of the breakdown-voltage with rising temperature, part of the measured bias-voltage range being a very low over-voltage, attributes to this effect. In order to reliably measure beyond an overvoltage of 2.5V in the lower range, the noise would need to be improved.
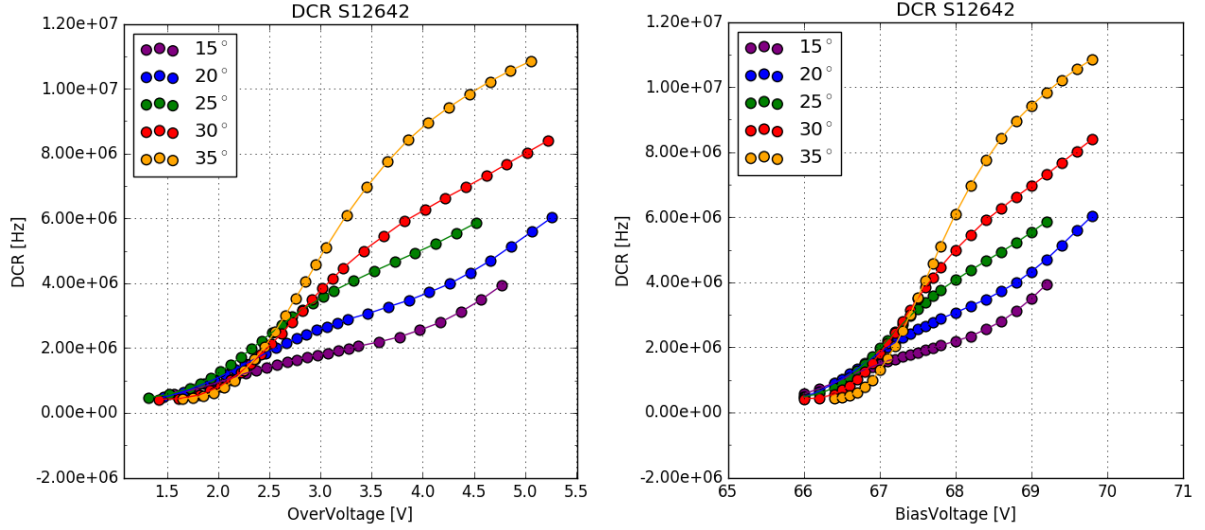
Figure 4: Dark Count Rate of the HPK S12642 pixel, plotted against over- , bias-voltage and temperature.

1.1.3 Optical Cross Talk

The Optical Cross Talk should be linear and independent from temperature. This is confirmed for HPK S12642. Minor diviations from that are probably due to slight errors in the breakdown-voltage calculation from the gain regression line. The diviation for 30° C and 35° C below an over-voltage of 2V stems from the way the gain regression line is used to calculate both Dark Count Rate and Optical Cross Talk. At higher temperatures the lower voltage range is dominated by noise, so using the gain regression line to calculate the Optical Cross Talk at those low voltages leads to the visible effect of the first few datapoints of 30° C and 35° C. The deviations between the different groups results at 25° C (green) are caused by 4 major contributions. Firstly the difference in the tested device. While I take measurements on 4 3mm by 3mm pixels electricaly tied together, the way the device will later be implemented into CHEC-S, the groups in the US and Hamamatsu Photonics are likely to run tests on 1 3mm by 3mm pixel only. Secondly I suspect a difference in amplification and shaping electronics. The measurements I conducted as well as the measurements of Leicester are done with the same shaper and buffer configuration. The difference here is, thirdly, my measurements are done with dark counts only, while measurements in Leicester are conducted with a pulsed light source and reading out timed windows. This causes the results from Leicester to be difficult to compare against, their surface temperature of the SiPM is likely much higher than 25° C, and thus, a misinterpreted breakdown-voltage at 25° C causes a shift of the Optical Cross Talk to the right. Lastly the difference in actual data taking and analysis procedure must be mentioned, also this is only of minor concern, as we will see with other measured devices.
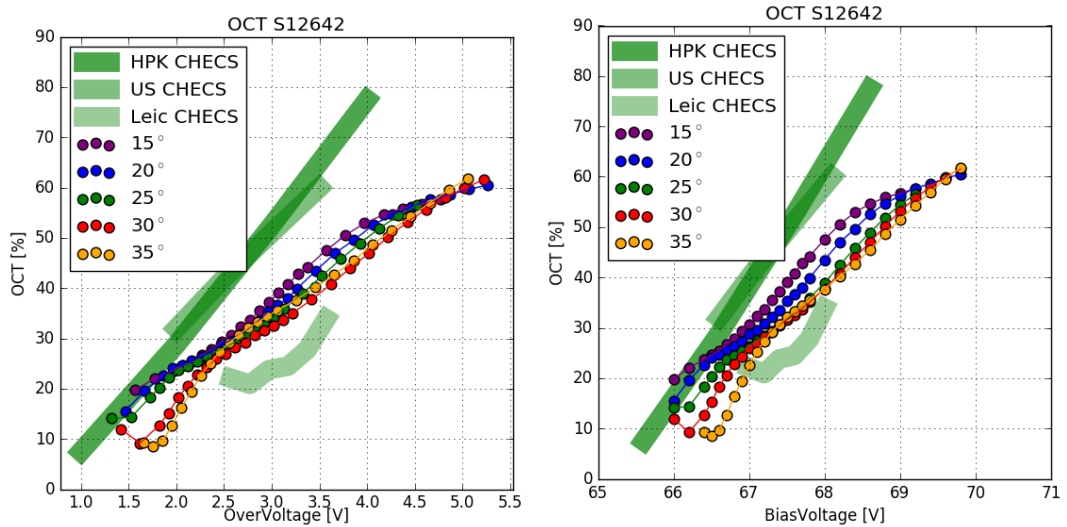

Figure 5: Dark Count Rate of the HPK S12642 pixel, plotted against over- , bias-voltage and temperature.

1.2 Hamamatsu LCT5 50μm 6mm

The Silicon Photomultiplier designated HPK S13360 6050CS is one of the most promising candidates for later usage in CHEC-S. It has a pixelsize of 6mm^2 with a cellsize of 50μm, therefore tests are done with a single pixel only, in contrast to measurements done on S12642. The layout of the single pixle test device made external amplification necessary. I used a minicircuits PreAMP Sn XXXXX, which was supplied with 13V during this test. Shaping of the pulse is conducted by a modified CHEC-S shaper, specifications can be found in chapter

Figure 6: HPK S13360 6050CS pixel / PreAMP pic will be updated

XXXXX. Even though the pulse shape fig(7) makes the pulses appear much harder to analyse, the possibility of events occuring during the ringing window. This assumption proved untrue, due to the devices low Dark Count Rate and Optical Cross Talk.
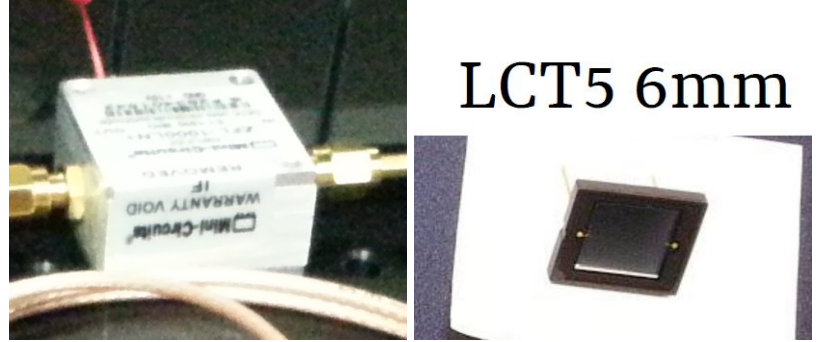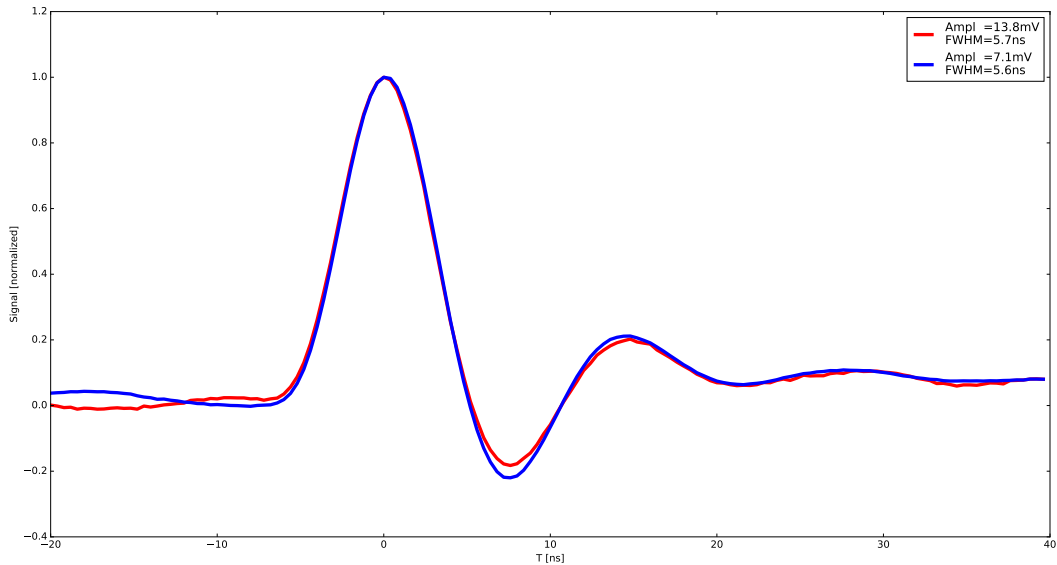

Figure 7: The average pulse shape of the 1photoelectron in blue and the 2photoelectron pulse in red of HPK S13360 6050CS at 25° C and at point of operation. Both pulses have a FWHM of around 5ns and ring for approximately 20ns with an undershoot of 20%.

1.2.1 Gain

The gain of the LCT5 50μm 6mm device is clearly linear with some minor outliers at 30°C. The same effect as with S12642 is visible at 35°C, again counting noise peaks as 1p.e. peaks, resulting in an apparent lowering of the gain and the slope changing over into a plateau. In Figure(17)(left) the gain is shown, plotted against over-voltage. It is still dependant on temperature, but due to reliable breakdown-voltage calculation, the spread is much smaller than, if plotted against bias-voltage. The same conversion is done to transform relative gain into an absolute gain with sensible units.
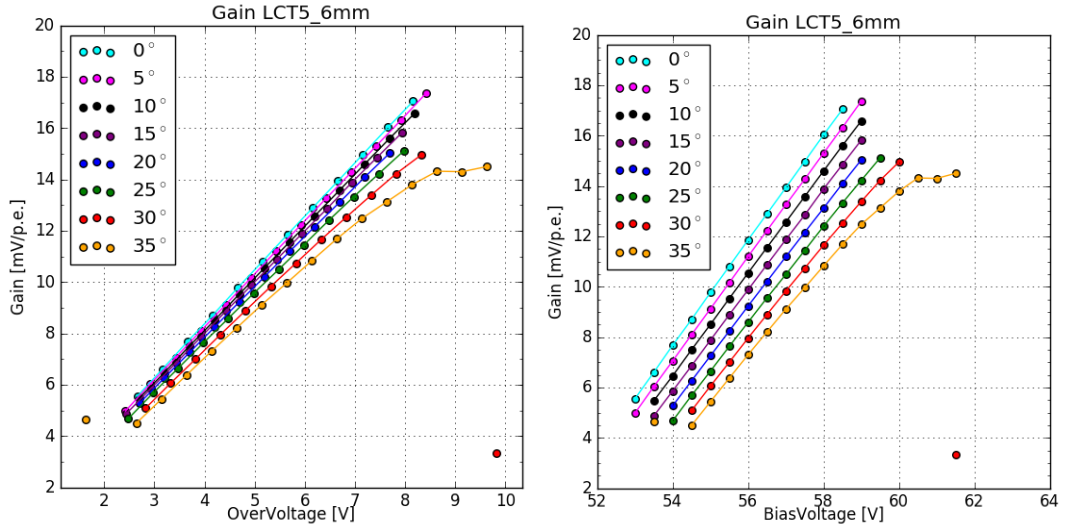
Figure 8: Gain of the HPK S13360 pixel, plotted against over- , bias-voltage and temperature.

1.2.2 Dark Count Rate

The Dark Count Rate of two similar HPK S13360 devices is shown in Figure(9). The bars show the difference between the two devices, the results of one device is used as a reference, while the deviation is illustrated with the filled bar. The Dark Count Rate of HPK S13360 followes the expected behaviour, mostly linear in the significant range and rising with increasing temperature. Below an over-voltage of 2.5V my analysis struggles, I suspect the gain to be to low for my analysis to pick up pulses. Thus the regression line calculation is unreliable in this range. The turnup at high over-voltages is most prominent at 0°C(teal) after an over-voltage of 9V. This is also the point where the Optical Cross Talk rises very rapidly.
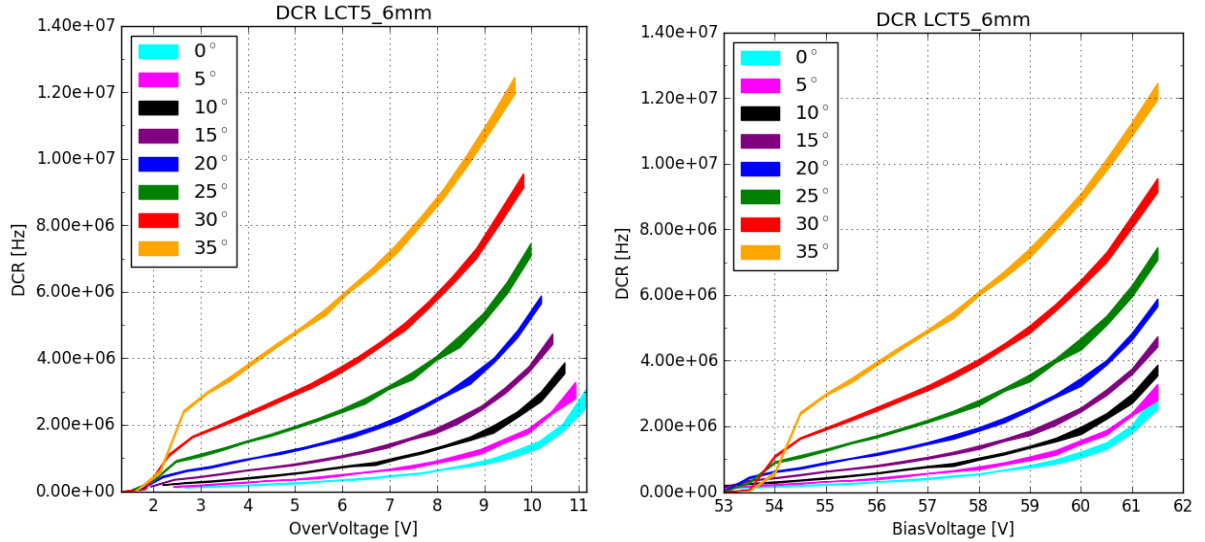

Figure 9: Dark Count Rate of the HPK S13360 pixel, plotted against over- , bias-voltage and temperature.

1.2.3 Optical Cross Talk

Compared to measurements on HPK S13360 done at the Nagoya University Japan 9 (faded green bar), I see a very strong correlation of the Optical Cross Talk in the over-voltage range between 2.5V and 9V. In contrast to my technique, using only dark counts, the measurements at Nagoya University followed a pulsed light source approach, reading out a time-window after the laser incident. Deviations below an over-voltage of 2.5V are expected, they are very likely caused by the regression line calculation being unreliable in this range due to the analysis method

struggling to pick up pulses using dark counts. Above an over-voltage of 9V, which is also the point of the turnup of the Dark Count Rate, the Optical Cross Talk is no longer linear and the deviation from the results of Nagoya University increase very rapidly. I suspect the rapid increase in both Dark Count Rate and Optical Cross Talk to be caused by the over-voltage reaching ranges, where interpretation of noise as a 1p.e. pulse becomes more likely. This, joint together with the usage of the Mini-Circuits amplifier supplied with 13V, makes false interpretation of noise as pulses even more likely. I suspect these two reasons in conjunction are responsible for both, the sudden rise of the Dark Count Rate as well as the deviation of the Optical Cross Talk from linearity and the results of Nagoya University, above over-voltages around 9V. In summary, the correlation between the two measurements, conducted by two different methods of data acquisition and analysis, is evident.
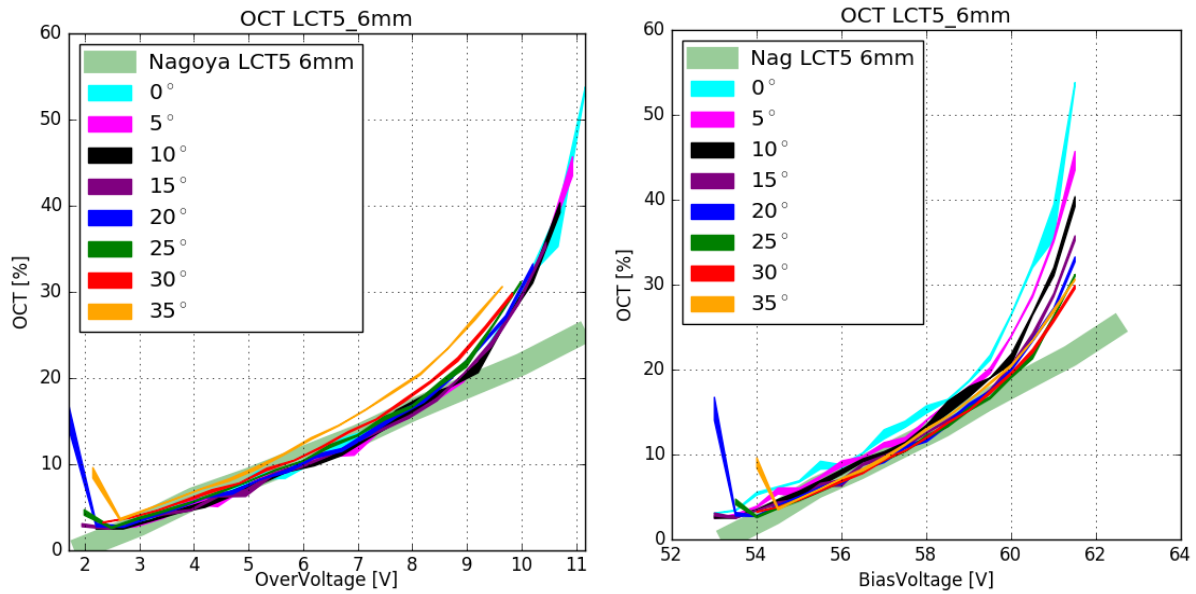

Figure 10: Optical Cross Talk of the HPK S13360 pixel, plotted against over- , bias-voltage and temperature.

1.3 Hamamatsu LCT5 75μm 7mm

XXXXXXXXXXXX is a larger prototype Silicon Photomultiplier of the same design as S13360. With an increase in cellsize to 75μm, the device gains a higher fillfactor than 50μm devices. The pixelarea is also expanded to 6.915mm^2, which will result in a larger FoV of GCT, see chapter (list of devices etc) !(maybe tom armstrongs simulations)!. It is also a single pixel test device, so external amplification is necessary. I used the same minicircuits PreAMP Sn XXXXX, supplied with 8V during this test. The signal is also shaped by a differently modified CHEC-S shaper, which results in a pulse shape similar to S12642, but with a much lower amplitude.
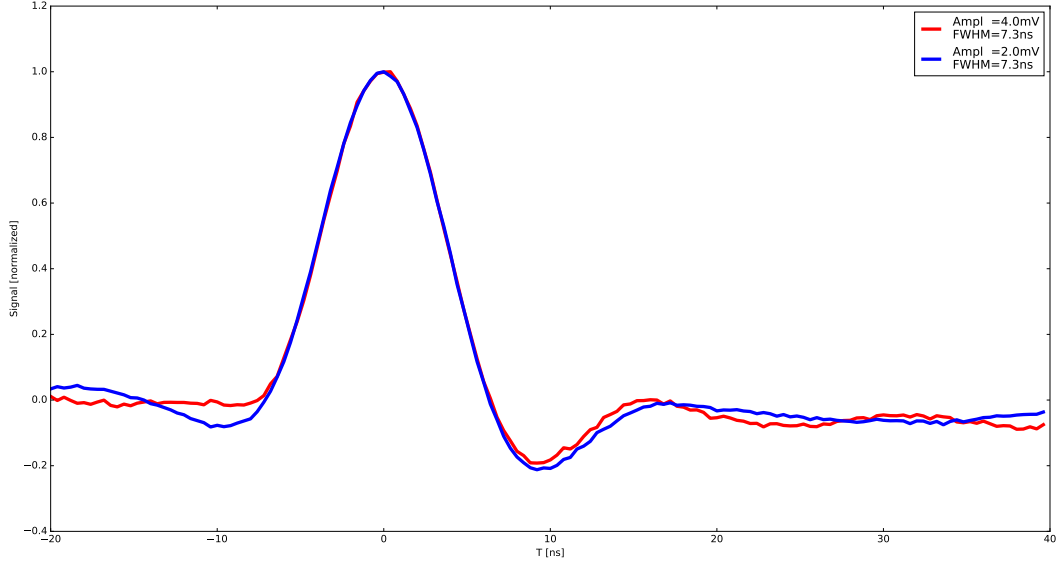

Figure 11: HPK LCT5 7mm pixel

Figure 12: The average pulse shape of the 1photoelectron in blue and the 2photoelectron pulse in red of HPK LCT5 7mm at 25° C and at point of operation. Both pulses have a FWHM of around 7ns and an undershoot of 20%, with no ringing.

1.3.1 Gain

Figure(13) shows the gain of the LCT5 7mm device. An second set of measurements is done for 25°C to extend the measured range. The first set of measurements covers the lower over-voltage range, where the low gain makes extenal amplification necessary. The same mini-circuits PreAMP (SNXXXXXXXXX) supplied with 8V was used during this test. I chose the lowest possible amplification of the PreAMP, so that reaching the point of saturation of the oscilloscope is as late as possible as the over-voltage rises. Saturation of the oscilloscope occurs due to the possibility of generating very large p.e. (>10p.e.) events at the higher over-voltages, which are saturating the input. Joint together, the LCT5 7mm device and the mini-circuits PreAMP at 8V reach this point at an over-voltage of ∼6V. In Figure(13) the results from the lower range measurement are displayed as the lower-range green line extending between an over-voltage of 1.6V to 5.4V.

The configuration for the second test removes the PreAMP from the setup, which makes the lower over-voltage range unaccesible, but extends the range to higher over-voltages. This configuration reaches the point of saturation at an over-voltage

Figure 13: Gain of the HPK LCT5 7mm pixel

of ∼8V. The higher range measurement results are displayed as the second green line (25°C) extending from 3.4V to 7.2V over-voltage in Figure(13). There is a clearly visible overlap of the two measurements between ∼3.4V and ∼5.4V . It also seems, that the gain dependency on temperature is reversed. While for all other devices, the gain lowers with rising temperatures, the LCT5 7mm device seems to show inversed behaviour. Behaviour confirmed in vs bias voltage plot.
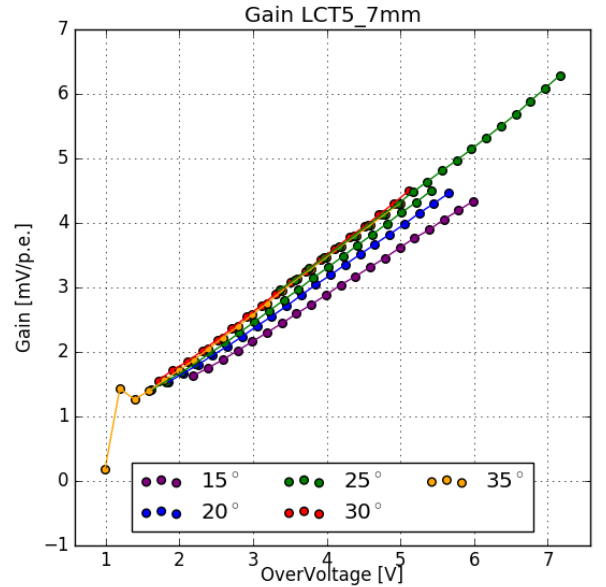
1.3.2 Dark Count Rate

The behaviour of the Dark Count Rate of the HPK LCT5 7mm device is shown in Figure(14) and is as expected, in contrast to the behaviour of the gain of LCT5 7mm, as discussed in section 1.3.1. It follows a linear progression in the relevant range and increases with rising temperature. I suspect the over-voltage range above ~2.5V to be relevant. The extended range measurement at 25°C confirms this behaviour. LCT5 7mm shows a linear Dark Count Rate over an over-voltage range of 4V. The faded green bar in Figure(14) shows results from measurements undertaken by the Department of Physics and Astronomy at the University of Catania. Those measurements were conducted on the exact same device, which is an important point, but with a different method of data acquisition and data analysis. LITTLE MORE DETAIL IN PROCESS. The correlation between the two experiments is evident, although there is differences in the acyquisition and analysis process. This is further proof for the relevancy of my analysis.
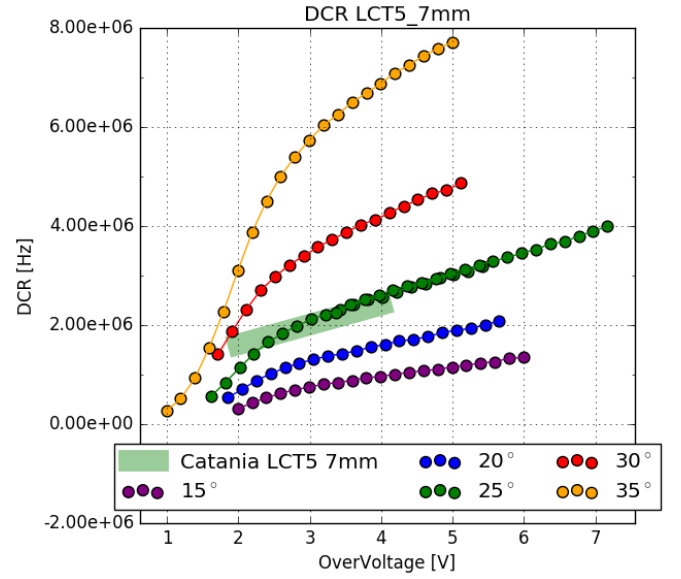

Figure 14: Dark Count Rate of the HPK LCT5 7mm pixel

1.3.3 Optical Cross Talk

The Dark Count Rate of two similar HPK S13360 devices is shown in Figure(15). The bars show the difference between the two devices, the results of one device is used as a reference, while the deviation is illustrated with the filled bar. Below an over-voltage of 2.5V my analysis struggles, I suspect the gain to be to low for my analysis to pick up pulses. Thus the regression line calculation is unreliable in this range. The turnup at high over-voltages is most prominent at 0°C(teal) after an over-voltage of 9V. This is also the point where the Optical Cross Talk rises very rapidly.
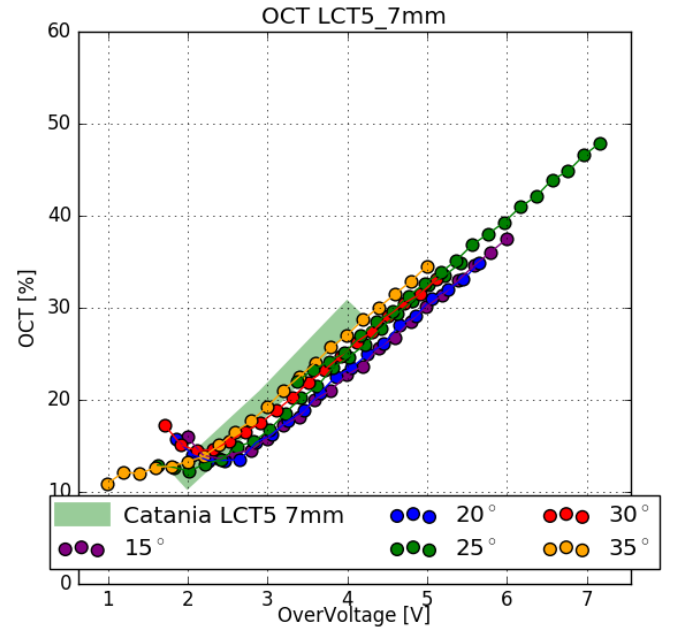

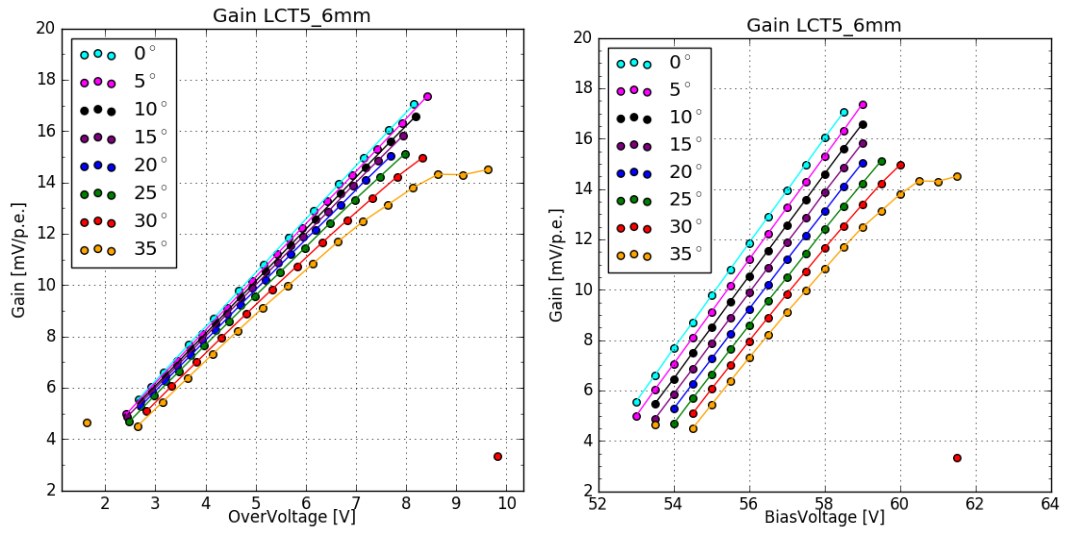Figure 15: Dark Count Rate of the HPK LCT5 7mm pixel

blank

ddd

Figure 17: Gain of the HPK S13360 pixel, plotted against over- , bias-voltage and temperature.

3 Appendices

1. Jim Hinton et al. Teraelectronvolt Astronomy Ann. Rev. Astron. Astrophys., 47:523

2. Julien Rousselle et al. Construction of a Schwarzschild-Couder telescope as a candidate for the Cherenkov Telescope Array: status of the optical system

3. CTA Consortium et al. Design Concepts for the Cherenkov Telescope Array

4. Teresa Montaruli et al. The small size telescope projects for the Cherenkov Telescope Array

5. The ASTRONET Infrastructure Roadmap ISBN: 978-3-923524-63-1

6. Jim Hinton et. al Seeing the High-Energy Universe with the Cherenkov Telescope Array Astroparticle Physics 43 (2013) 1-356

7. John Murphy SensL J-Series Silicon Photomultipliers for High-Performance Timing in Nuclear Medicine

8. A. N. Otte et al. Characterization of three high efficient and blue sensitive Silicon photomultipliers

9. http://astro.desy.de/gamma_astronomie/cta/medien/ueber_cta/index_ger.html

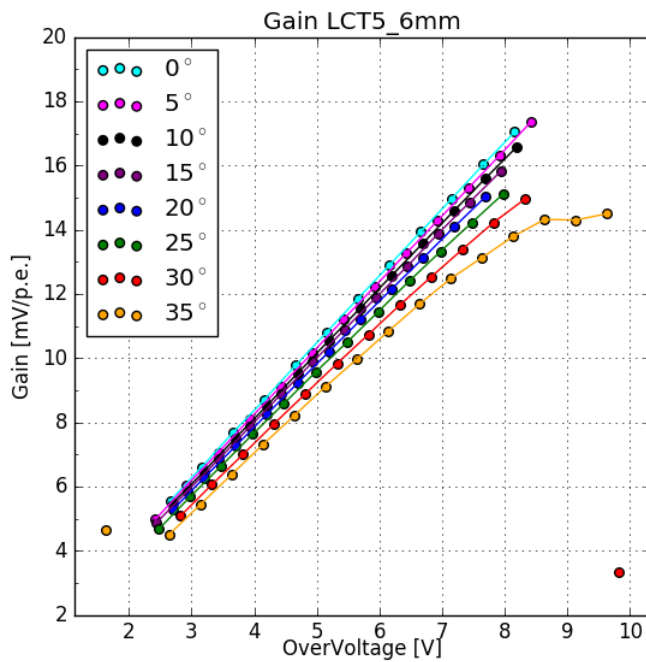10. http://www.ung.si/en/research/laboratory-for-astroparticle-physics/projects/cta/

Figure 16: HPK S13360 6050CS pixel / PreAMP pic will be updated